

## Transient analysis of organic electrophosphorescence: I. Transient analysis of triplet energy transfer

M. A. Baldo and S. R. Forrest

*Center for Photonics and Optoelectronic Materials (POEM), Department of Electrical Engineering and the Princeton Materials Institute, Princeton University, Princeton, New Jersey 08544*

(Received 3 January 2000; revised manuscript received 10 May 2000)

We examine triplet-exciton dynamics in several phosphorescent organic guest-host systems. In this first of two papers, transient studies are used to understand triplet energy transfer between molecules and also to ascertain the relative importance under electrical injection of charge trapping and direct exciton formation on phosphorescent guest molecules. As an example, we study the distribution of triplet excitons as they diffuse through amorphous films of tris(8-hydroxyquinoline) aluminum ( $\text{Alq}_3$ ). We find that triplet transport in  $\text{Alq}_3$  is dispersive, and for high concentrations of triplets we find an average lifetime of  $\tau = 25 \pm 15 \mu\text{s}$  and a diffusion coefficient of  $D_T = (8 \pm 5) \times 10^{-8} \text{ cm}^2/\text{s}$ . The understanding of the formation and transport of triplets in a host material is extended in the following paper [Phys. Rev. B **62**, 10 967 (2000)] to the study of nonlinearities in the electroluminescent decay of phosphorescent organic guest materials. Finally, we summarize the principle determinants of the efficiency of organic electrophosphorescent devices.

### I. INTRODUCTION

Phosphorescence in organic materials is distinguished from fluorescence by its origin in forbidden transitions that violate spin conservation.<sup>1</sup> The excitons responsible for phosphorescence and fluorescence are named after their spin multiplicity as triplets and singlets, respectively. Given that electrical excitation generates three triplets for every singlet exciton,<sup>2</sup> triplet properties are of interest, not least because of their application to organic optoelectronic devices.<sup>3</sup> However, triplet radiative decay rates are small and triplet decay can be difficult to observe, particularly at room temperature where nonradiative decay dominates. But by employing molecules with high phosphorescence efficiencies, transient electrophosphorescence may be used to observe the diffusion of triplets within a conductive organic host material, or it may give evidence for charge trapping and direct exciton formation on dopant molecules within the host. Thus, it provides a convenient tool for examination of energy transfer, either from one host molecule to another, or from the host to a dopant.<sup>4</sup>

We are concerned in this work with electrical excitation of thin amorphous organic films where a phosphorescent guest is dispersed within a conductive host material. Proceeding from exciton formation, we study the dynamics of triplets until the point of their radiative or nonradiative decay. In this paper (Paper I), the energy levels of a selection of guest and host materials are examined to determine whether excitons form primarily on guest molecules, or whether they are formed in the host and must diffuse to guest molecules where they are subsequently trapped. We identify examples of both systems and particularly study triplet diffusion in the well-known electron-transporting material tris(8-hydroxyquinoline) aluminum ( $\text{Alq}_3$ ). From the phosphorescent transient decays, we are able to estimate the  $\text{Alq}_3$  triplet-exciton diffusion coefficient and lifetime.

In the subsequent paper<sup>5</sup> (Paper II), we examine the dy-

namics of triplet excitons after they are localized on guest molecules by observing the effect of triplet concentration on the phosphorescent transients. It is found that interactions between triplets on adjacent molecules significantly affect the efficiency of electrophosphorescence, particularly at high luminescent intensities. We conclude by summarizing the properties of guest-host phosphorescent systems and possible methods for minimizing nonradiative triplet losses.

In this paper, we outline the fundamental principles of triplet energy transfer in Sec. II. The experimental methods are described in Sec. III and the chemical structures and excitonic energy levels of the various organic host and guest materials are presented in Sec. IV. We isolate the molecular species upon which excitons form using transient analysis in Sec. V, and in Sec. VI we examine a guest-host combination where triplet diffusion is significant. Conclusions are presented in Sec. VII.

### II. TRIPLET ENERGY TRANSFER

Four processes determine the overall efficiency of energy transfer between a host and a guest molecule: the rates of exciton relaxation on the guest and host,  $k_G$  and  $k_H$ , respectively, and the forward and reverse triplet transfer rates between guest and host,  $k_F$  and  $k_R$ , respectively. The rate equations, in the absence of exciton-formation processes, are

$$\begin{aligned} \frac{dG}{dt} &= -k_G G - k_R G + k_F H, \\ \frac{dH}{dt} &= -k_H H - k_F H + k_R G, \end{aligned} \quad (1)$$

where  $G$  and  $H$  are the densities of guest and host triplet excitons. The solutions to Eq. (1) are biexponential decays, of the form

$$G, H = A_1 \exp[-k_1 t] + A_2 \exp[-k_2 t], \quad (2)$$

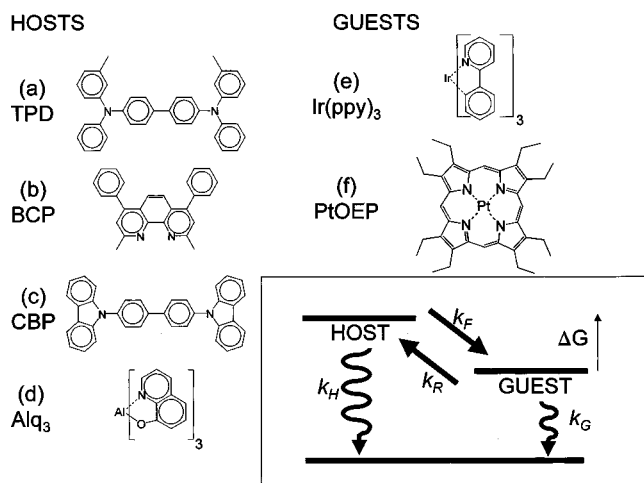


FIG. 1. The molecular structures of the materials studied: (a) TPD (*N,N'*-diphenyl-*N,N'*-bis(3-methylphenyl)-[1,1'-biphenyl]-4,4'-diamine), (b) BCP (2, 9-dimethyl-4,7-diphenyl-1, 10-phenanthroline), (c) CBP (4,4'-*N,N'*-dicarbazole-biphenyl), (d) Alq<sub>3</sub> tris(8-hydroxyquinoline) aluminum, (e) Ir(ppy)<sub>3</sub> *fac* tris(2-phenylpyridine) iridium, and (f) PtOEP 2, 3, 7, 8, 12, 13, 17, 18-octaethyl-21*H*,23*H*-porphine platinum(II). Inset: Triplet dynamics in a guest-host system: the rates of forward and back transfer,  $k_F$  and  $k_B$ , respectively, are determined by the Gibbs's free energy change ( $\Delta G$ ) and the molecular overlap; also significant are the rates of decay from the guest and host triplet states, labeled  $k_G$  and  $k_H$ , respectively.

where  $A_1$  and  $A_2$  are determined by the initial conditions, and the characteristic decay rates  $k_1$  and  $k_2$ , are given by

$$k_1, k_2 = \frac{k_F + k_R + k_H + k_G}{2} \times \left( 1 \pm \sqrt{1 - \frac{4(k_G + k_R)(k_H + k_F) - 4k_F k_R}{(k_F + k_R + k_H + k_G)^2}} \right). \quad (3)$$

The energy-transfer processes are shown schematically in the inset of Fig. 1. It is apparent that to maximize guest phosphorescence, we require that either  $k_G \gg k_H$  or  $k_F \gg k_R \gg k_H$ .

Situations where  $k_G \gg k_H$  enable efficient phosphorescence by minimizing losses in the host and can be realized by employing a host material with a long triplet lifetime ( $k_H$  small). As shown below, efficient phosphorescence from the guest is possible even if its triplet energy is higher than that of the host ( $\Delta G > 0$  in Fig. 1), in which case guest phosphorescence may be slower than the natural phosphorescent radiative lifetime. The second case ( $k_F \gg k_R \gg k_H$ ) maximizes the population of guest triplets and avoids any losses that may occur on the host.

Examination of the phosphorescent transient decay yields the sum of the radiative and nonradiative rates of triplet decay, or  $k_H$  or  $k_G$  for the host and guest, respectively. The nonradiative rate of triplet decay is strongly enhanced as temperature increases; thus many materials exhibit little or no phosphorescence at room temperature. For these materials, more complex methods such as transient absorption spectroscopy,<sup>6</sup> must be employed to determine triplet life-

times at room temperature. It is also possible to use decay rates measured at low temperature to estimate the room-temperature triplet lifetimes.

To understand the origin of  $k_F$  and  $k_R$  we must first examine the theory of triplet energy transfer. Dexter<sup>7</sup> found that exchange interactions permit exciton hops from one molecule to the next with no change in spin. In such a process, triplet transfer may be thought of as a simultaneous transfer of an electron and a hole. Indeed, Closs *et al.*<sup>8</sup> have studied triplet energy transfer in molecules of the general form *D*-Sp-*A*, where *D* is 4-biphenyl, *A* is 2-naphthyl, and the spacer molecules (Sp) are trans-decalin and cyclohexane with different regiochemical and stereochemical attachments. With correction of the reorganization energy and comparison of the rates of triplet transfer with those of electron and hole transfer, the triplet transfer rate has been demonstrated<sup>8</sup> to be related to the product of the electron and hole transfer rates calculated from Marcus theory.<sup>8-10</sup>

Applicable to systems with very weak overlap between the electronic orbitals of the reactants, Marcus theory recognizes that the rate-limiting step is not the electron transfer itself, but rather the formation of the activated complex that precedes the transfer. This is a reflection of the Franck-Condon principle: during an electronic transition, the electronic motion is so rapid that the atomic configuration of the reactant and product states is unchanged. The most probable activated complex is determined by minimizing its free energy of formation ( $G$ ) under the restriction that the total energy of the complex is unchanged during the electron transfer.

This reasoning leads to a transfer probability ( $k$ ) of the form<sup>10</sup>

$$k = \sqrt{\frac{4\pi^3}{h^2 \lambda k_B T}} |M_{DA}|^2 \exp\left[-\frac{(\Delta G + \lambda)^2}{4\lambda k_B T}\right], \quad (4)$$

where the matrix element mixing donor and acceptor states is  $M_{DA}$ ,  $h$  is Planck's constant,  $k_B$  is Boltzmann's constant, and  $T$  is the temperature. If the transfer occurs with no change in free energy ( $\Delta G = 0$ ) or in the atomic configuration of the reactants, then the energy barrier is  $\lambda$  (assumed to be the same in both forward and reverse transfer directions). But for small changes in the free energy, Marcus transfer via an activated complex behaves similar to an Arrhenius barrier of approximately  $\lambda/4$ . As the difference in the donor and acceptor triplet energies increases, the rate also increases until resonance is reached. For large differences the transfer rate decreases, giving the "Marcus inverted region."

In order to estimate  $\Delta G$ , we measure the relaxed triplet state energies of both the donor and acceptor molecules using their phosphorescent spectra. As discussed in Sec. IV, due to the low probability of radiative triplet transitions, spectra must generally be obtained by minimizing nonradiative transitions at low temperature. The spectra are characterized by several vibronic overtones in the ground state manifold. The energy difference between the first excited triplet state and the ground state is estimated from the highest energy transition observed in phosphorescence.

In addition to the energy considerations of Eq. (4), Dexter transfer requires that the combined spin of the participating molecules be conserved during energy transfer. For example, triplet transfer may follow:

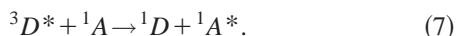


where  $D$  is the donor and  $A$  the acceptor. Triplet and singlet states are represented by superscript 3 and 1, respectively, and the asterisk signifies an excited state. Note that singlet states in the host may also be transferred to the guest via the Dexter mechanism; however, if the spectral overlap is sufficient, then typically the long-range competing mechanism of dipole-dipole or Förster energy transfer predominates.<sup>11</sup> Singlet transfer is simply



After transfer, the singlets on the organometallic phosphorescent guest molecules studied in this work rapidly intersystem cross to the triplet state. This is due to the presence of a heavy atom that introduces spin-orbit coupling, breaking the spin-selection rules.

Another energy-transfer mechanism is Förster energy transfer from the triplet state of the donor to the singlet state of the acceptor, following



This process may be very efficient if the donor is phosphorescent.<sup>12</sup> It may be employed to transfer triplet states to the singlet state of the acceptor,<sup>12</sup> but we observe it here by dispersing a phosphorescent guest into a second phosphorescent host. Unlike triplet-triplet transfer, the donor and acceptor molecules are well coupled in Förster transfer; hence the rate depends on the overlap of donor emission and acceptor absorption.

### III. EXPERIMENTAL TECHNIQUES

The phosphorescent spectra of our materials were measured to obtain their triplet energy levels. Luminescence was measured from 2000-Å-thick films of each organic material, following ~1-Hz excitation with a 500-ps pulse from a N<sub>2</sub> laser at a wavelength of  $\lambda = 337$  nm. Delayed photoluminescence (PL) was isolated using a streak camera and separated into delayed fluorescence and phosphorescence. The delayed fluorescence originates from singlets produced by triplet-triplet annihilation<sup>1</sup> and is easily distinguished from phosphorescence since it scales with the square of pump intensity.

The electroluminescent (EL) properties of various organic films were studied by incorporating them as host materials within organic light emitting devices (OLED's). It is characteristic of electrophosphorescence for the peak efficiency to occur at low current densities ( $J < 0.1$  mA/cm<sup>2</sup>), necessitating the minimization of leakage currents that do not contribute to luminescence. Substrate cleanliness and material purity were found to be crucial in obtaining an accurate measurement of efficiency at low current density. Glass substrates precoated with a 1400-Å-thick layer of indium tin oxide (ITO) were exposed to a uv/ozone flux for 5 min after sequential solvent cleaning with trichloroethylene, acetone, and isopropanol. The organic source materials (see Fig. 1) were purified by train sublimation at least once before they were loaded into a high vacuum ( $10^{-6}$  Torr) thermal evaporation chamber.<sup>13</sup> For guest-host combinations, the doping fractions quoted are mass percentages determined during

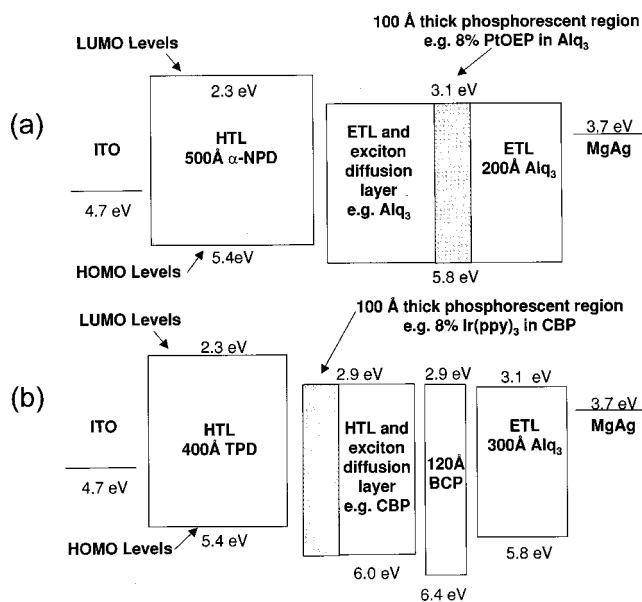


FIG. 2. The structure of the electroluminescent devices used to observe the transient response of triplet diffusion in organic host materials. Electron- and hole-transport layers are labeled ETL and HTL, respectively. The highest occupied molecular orbital (HOMO) obtained for each material corresponds to its ionization potential (IP). The lowest unoccupied molecular orbital (LUMO) is equal to the IP plus the optical energy gap, as determined from absorption spectra. Relative alignments of the energies in the fully assembled devices will differ from those shown. Two devices are shown: in (a) the host preferentially transports electrons and the exciton formation zone is at the interface between the host and  $\alpha$ -NPD, in (b) the host preferentially transports holes and exciton formation is at the interface between the host and BCP. In both devices triplets are forced to diffuse through the host before reaching a phosphorescent region, created by doping a narrow (~100-Å) layer of the host with a phosphorescent dye. Singlets formed during electrical excitation cause fluorescence within the host, thus triplet dynamics are reflected in the delay between fluorescence and phosphorescence.

deposition by individual quartz-crystal thickness monitors positioned in the vacuum chamber adjacent to the guest source and the substrate.

The materials used are (a)  $N,N'$ -diphenyl- $N,N'$ -bis(3-methylphenyl)-[1,1'-biphenyl]-4,4'-diamine (TPD), (b) 2,9-dimethyl-4,7-diphenyl-1,10-phenanthroline (bathocuproine or BCP), (c) 4,4'- $N,N'$ -dicarbazole-biphenyl (CBP), (d) Alq<sub>3</sub>, (e) *fac* tris(2-phenylpyridine) iridium [Ir(ppy)<sub>3</sub>]<sup>14</sup> and (f) 2,3,7,8,12,13,17,18-octaethyl-21*H*,23*H*-porphine platinum(II) (PtOEP). Of these materials, TPD and CBP are predominantly hole-transport, and Alq<sub>3</sub> and BCP are electron-transport materials. Two phosphors are also employed as guests: Ir(ppy)<sub>3</sub>, which emits at ~510 nm with a phosphorescent lifetime of ~0.4  $\mu$ s,<sup>14</sup> and PtOEP, which emits at 650 nm with a phosphorescent lifetime of ~100  $\mu$ s.<sup>3</sup>

Two test structures were made, depending on the conductivity of the host material. If it is preferentially an electron transporter, then it is used as an electron transport layer (ETL) and employed in the structure of Fig. 2(a). Of the host materials used, Alq<sub>3</sub> and BCP films may serve as an ETL; the remaining materials are predominantly hole conductors and can be used in hole-transport layers (HTL's). For these

materials, a wide-energy-gap hole and exciton-blocking material are required to contain the excitations within the HTL. For this purpose, we used BCP in structures shown in Fig. 2(b). It has previously been shown<sup>15</sup> that BCP conducts electrons but blocks holes from entering the ETL.

For electroluminescent devices employing Alq<sub>3</sub> as the host, the exciton-formation zone is located at the interface of the HTL and Alq<sub>3</sub>. In the case of HTL host materials, the exciton-formation zone is at the interface between the HTL and BCP. To study exciton diffusion, undoped layers of the host material were inserted between the exciton-formation interface and a phosphorescent layer. As shown in Fig. 2, triplets are forced to diffuse through this undoped zone before being captured by the doped luminescent, or “triplet sensing,” layer. Also shown in Fig. 2 are proposed energy levels for the host and guest materials. The electron energy levels referenced to vacuum are indicated by the lowest unoccupied molecular orbital (LUMO) and the energy levels of holes are given by the highest occupied molecular orbitals (HOMO), as determined from the ionization potential for each material.<sup>16</sup> Note that we have assumed that the HOMO-LUMO gap is equal to the optical energy gap, as determined from absorption spectra. Under this assumption, the LUMO does not necessarily serve as the lowest conduction level for mobile electrons. Although not shown here, charge redistributions and polarization effects at the heterointerfaces are expected to alter the relative energy-level alignments when differing materials are brought into contact.<sup>17</sup>

The devices were fabricated by thermal evaporation of the source materials under high vacuum ( $\sim 10^{-6}$  Torr). In successive evaporations, a hole-transport material was deposited on a precleaned<sup>3</sup> glass substrate coated with ITO. This is followed by deposition of the host material. If the host is also an HTL, a 120-Å-thick BCP blocking layer was employed. All devices employed an Alq<sub>3</sub> ETL to separate the emissive region from the 1000-Å-thick 20:1 Mg:Ag cathode, thereby positioning the luminescent region more favorably within the microcavity created by the metal cathode.<sup>18</sup> The devices were completed by depositing a 500-Å-thick layer of Ag to protect the Mg-Ag cathode from oxidation. Metal depositions were defined by a shadow mask with an array of 1-mm-diam openings.

Transient measurements were obtained by applying a narrow (200-ns) voltage pulse to the device under test and coupling the emission into a streak camera. This pulse width is chosen to be less than the radiative rate of the phosphors and larger than the charging time of the OLED, which for a 50-Ω load and a typical capacitance of 1 nF is  $\sim 50$  ns. In some cases, the sample was placed under  $-10$  V reverse bias following the electrical pulse. External EL quantum efficiency measurements were made by placing the completed OLED directly onto the surface of a calibrated silicon photodetector and capturing every photon emitted in the forward (viewing) direction.<sup>19</sup> All measurements were performed in air, except for those at low-temperature which were performed in an evacuated closed-cycle refrigerator.

#### IV. PHOSPHORESCENT PROPERTIES OF THE MATERIALS UNDER STUDY

The host materials, TPD, CBP, and Alq<sub>3</sub> are fluorescent and possess small or negligible phosphorescence at room

temperature due to competing thermally activated nonradiative decay processes. In addition to intramolecular pathways, these nonradiative processes include triplet diffusion to defect sites followed by dissipative transitions. Reducing the temperature slows the rate of phonon-assisted decay and triplet diffusion, and the phosphorescent PL spectra for TPD, CBP, and BCP at  $T = 10$  K are shown in Fig. 3 together with the room-temperature spectra of PtOEP and Ir(ppy)<sub>3</sub>. After extended sampling, it was possible to obtain the room-temperature phosphorescent spectra and lifetimes for TPD and CBP. These measurements were possible because the triplet lifetimes of these materials are relatively long at room temperature:  $200 \pm 50 \mu\text{s}$  and  $>1$  s, respectively. In fact, under ultraviolet excitation, weak orange CBP phosphorescence is visible to the naked eye at room temperature. In contrast, the triplet lifetime of BCP decreases rapidly as temperature increases from  $\sim 1$  s at 10 K to  $<10 \mu\text{s}$  at room temperature, although we note that short triplet lifetimes may be dominated by energy transfer to physical or chemical defects.

No phosphorescence was observed from Alq<sub>3</sub> even at temperatures as low as  $\sim 10$  K. In their study of hydroxyquinoline complexes, Ballardini *et al.*<sup>20</sup> were similarly unsuccessful in observing phosphorescent emission from Alq<sub>3</sub>, although they could observe the phosphorescent spectra of hydroxyquinoline complexes of Pb, Bi, Rh, Ir, and Pt. These latter materials all show triplet emission at 590–650 nm and while we cannot be certain that the triplet energy of Alq<sub>3</sub> also lies within this range, it seems likely that it is significantly red-shifted from the spectra of the other host materials in Fig. 3.

The triplet energies (measured from the highest energy peak of the PL spectra) and decay lifetimes are summarized in Table I. From the triplet energies, the free energy change  $\Delta G$  on triplet transfer can be calculated for combinations of host and guest materials. Given the guest materials PtOEP and Ir(ppy)<sub>3</sub>, it is possible to categorize several host and guest combinations based on the magnitude and sign of  $\Delta G$  (see Fig. 1):

(i)  $\Delta G \ll 0$ . Example guest-host combinations where triplets on guest molecules are strongly confined include PtOEP in CBP and PtOEP in TPD. In these cases, the guest and host triplet energies are nonresonant; hence although  $k_F \gg k_R$ , both rates are much smaller than their resonance maxima.

(ii)  $\Delta G < 0$ . There are two examples of weak triplet confinement: PtOEP in Alq<sub>3</sub> and Ir(ppy)<sub>3</sub> in CBP. Here  $k_F > k_R$ , the system is close to resonance, and significant populations of both guest and host triplets exist.

(iii)  $\Delta G > 0$ . In films of Ir(ppy)<sub>3</sub> in TPD the triplets are expected to reside primarily on the host with  $k_R > k_F$ .

(iv)  $\Delta G \gg 0$ . Here, Ir(ppy)<sub>3</sub> in Alq<sub>3</sub> exhibits<sup>14</sup> extremely inefficient phosphorescence due to Alq<sub>3</sub> quenching of Ir(ppy)<sub>3</sub> triplets (corresponding to  $k_R \gg k_F$ ), and will not be considered further.

#### V. ELECTROLUMINESCENT TRANSIENT DATA

Together with the energetic considerations outlined above, the efficiency of phosphorescence depends on the creation rates of triplets on the host and guest species. For example, if the bulk of excitons are formed on the guest mo-

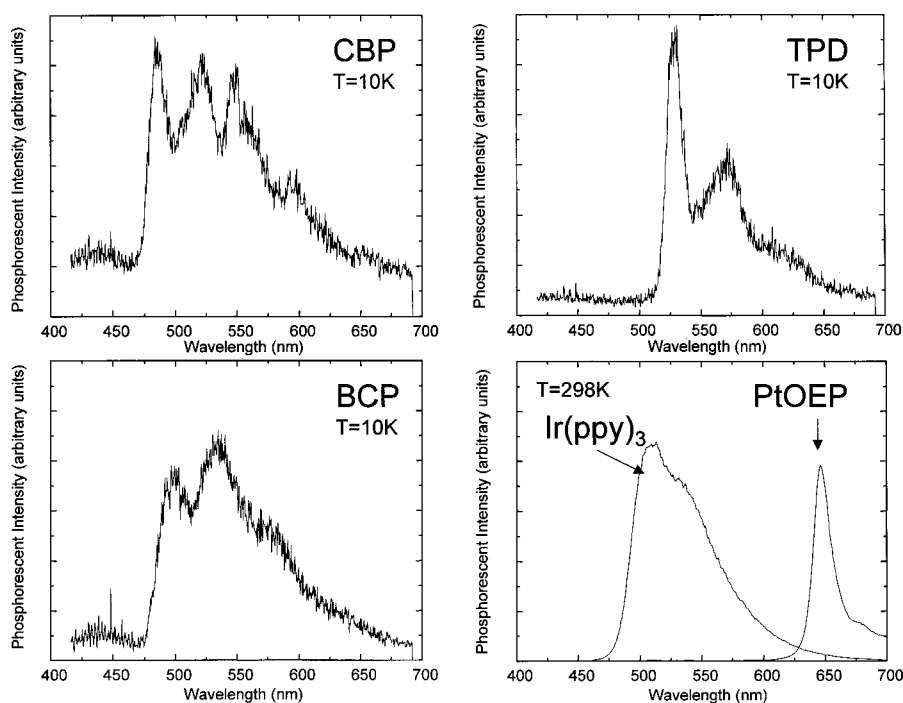


FIG. 3. The phosphorescent spectra of TPD, BCP, CBP, and  $\text{Ir}(\text{ppy})_3$  together with PtOEP. The spectra for TPD, BCP, and CBP were recorded at  $T = 10\text{ K}$  due to their very low phosphorescent efficiency at room temperature. These materials also exhibited significant delayed fluorescence due to singlet generation after triplet-triplet annihilation, but these spectra were recorded 200 ms after excitation, after which time the fluorescence is negligible. Due to strong singlet-triplet mixing, the spectra for PtOEP and  $\text{Ir}(\text{ppy})_3$  could be obtained at room temperature. Not shown is the phosphorescence spectrum of  $\text{Alq}_3$ , as its phosphorescent efficiency is negligible at  $T = 10\text{ K}$ . However, as discussed in the text, we expect that its triplet energy is approximately 2.0 eV.

molecular species, then efficient phosphorescence may be possible even though triplets are only weakly confined. Therefore, to understand a particular electrophosphorescent guest-host system, we need to know the site of exciton formation.

This may be determined by analysis of the phosphorescent transients. As discussed in Sec. III, the phosphorescent zone in the structures of Fig. 2 can be displaced from the exciton formation zone, forcing triplets to diffuse across several hundred Ångströms of organic material prior to recombination. To measure the diffusion time, we first apply a short electrical pulse and generate singlet and triplet excitons

TABLE I. Material triplet energies and room-temperature triplet lifetimes.

Material	Triplet energy ( $\pm 0.1\text{ eV}$ )	Triplet lifetime
PtOEP	1.9	$110 \pm 10\ \mu\text{s}^a$
$\text{Ir}(\text{ppy})_3$	2.4	$0.8 \pm 0.1\ \mu\text{s}^b$
CBP	2.6	$> 1\ \text{s}$
BCP	2.5	$< 10\ \mu\text{s}$
TPD	2.3	$200 \pm 50\ \mu\text{s}$
$\text{Alq}_3^c$	2.0	$25 \pm 15\ \mu\text{s}$

<sup>a</sup>6% PtOEP doped in CBP, photoexcitation density  $< 10^{17}\text{ cm}^{-3}$ .

<sup>b</sup>6%  $\text{Ir}(\text{ppy})_3$  doped in BCP, photoexcitation density  $< 10^{17}\text{ cm}^{-3}$ .

<sup>c</sup>The  $\text{Alq}_3$  triplet energy is inferred from the phosphorescent spectra of related hydroxyquinoline complexes of Pb, Bi, Rb, and Ir (Ref. 20). The triplet lifetime is calculated from the diffusion measurements in Sec. V.

at the ETL/HTL interface. The formation of excitons follows the current transient and is observed by measuring transient fluorescence from singlets in the host material. Then after the electrical excitation has ceased, the delay between the fluorescence and the onset of phosphorescence is measured. Either charge or triplet diffusion may be responsible for the delay, but charge diffusion can be effectively “turned off” by applying reverse bias following the excitation pulse to discharge traps and sweep out the remaining charge.<sup>4</sup> Therefore, if similar delayed phosphorescence is observed in the presence and absence of reverse bias, then charge trapping on guest molecules must be significant.

Since the probability of triplet transfer is proportional to the product of the electron and hole transfer probabilities,<sup>8</sup> we would expect that triplet diffusion should occur at a slower rate than charge transport. However, even in cases where charge diffusion dominates the phosphorescent decay, we cannot discount the possible additional presence of triplet diffusion. For example, the delay in triplet transport is limited by the triplet lifetime, which may be shorter than the charge-diffusion time. Or, the various species may diffuse over different distances prior to localization on a phosphorescent molecule. Hence, in those systems where delayed phosphorescence is eliminated by reverse bias, we can conclude that charge trapping is significant, but we cannot exclude the possibility that rapid triplet diffusion also occurs.

In Fig. 4 the transient responses of four electrophosphorescent material systems are shown. The device in Fig. 4(a) [cf. Fig. 2(a)] consists of a 600-Å-thick  $\text{Alq}_3$  diffusion layer and a phosphorescent sensing layer of 8% PtOEP doped in  $\text{Alq}_3$  (8% PtOEP: $\text{Alq}_3$ ). The PtOEP: $\text{Alq}_3$  transients clearly

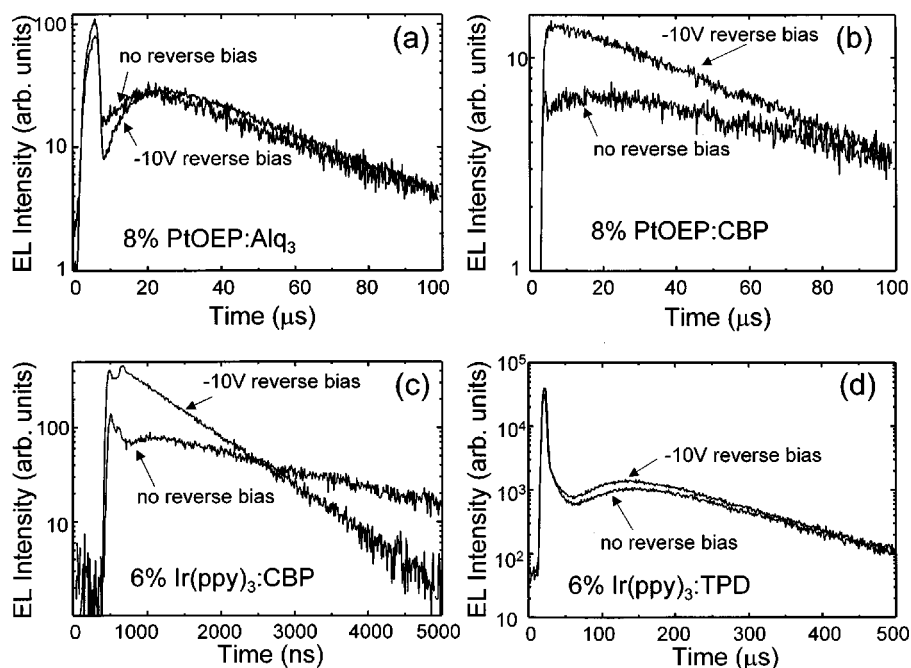


FIG. 4. The transient response of four archetypal phosphorescent guest-host systems. The PtOEP transients were recorded at  $\lambda = 650 \pm 10$  nm and the Ir(ppy)<sub>3</sub> transients at  $\lambda = 530 \pm 30$  nm. The initial peaks in the transient decays are host fluorescence at the wavelengths of interest; they mark the formation of singlet excitons. Triplet energy transfer is demonstrated in (a) by PtOEP:Alq<sub>3</sub>. These transients exhibit strong delayed phosphorescence due to triplet diffusion in Alq<sub>3</sub> and also show minimal change when reverse bias is applied to empty traps. This device had a 600-Å-thick Alq<sub>3</sub> diffusion layer and a phosphorescent sensing layer of 8% PtOEP in Alq<sub>3</sub>. However, in (b) we observe that PtOEP:CBP fails to show delayed phosphorescence when reverse bias is applied, indicating that charge trapping on PtOEP is significant. This device had a 400-Å-thick CBP diffusion layer and a phosphorescent sensing layer of 8% PtOEP in CBP. Similarly, in (c) the transient response of Ir(ppy)<sub>3</sub>:CBP also exhibits charge trapping on Ir(ppy)<sub>3</sub>. This device had a 500-Å-thick CBP diffusion layer and a phosphorescent sensing layer of 6% Ir(ppy)<sub>3</sub> in CBP. Energy transfer to Ir(ppy)<sub>3</sub> is observed in Ir(ppy)<sub>3</sub>:TPD (d). Here, the observed lifetime of Ir(ppy)<sub>3</sub> is 15  $\mu$ s, significantly longer than its natural radiative lifetime of 1  $\mu$ s. Taken together with the apparent absence of charge trapping on Ir(ppy)<sub>3</sub> in TPD, this long lifetime indicates that energy transfer from TPD to Ir(ppy)<sub>3</sub> might be the rate-limiting step in Ir(ppy)<sub>3</sub> phosphorescence. This device had a 200-Å-thick TPD diffusion layer and a phosphorescent sensing layer of 6% Ir(ppy)<sub>3</sub> in TPD. Note that the intensity of each transient measurement is arbitrary.

exhibit delayed phosphorescence due to triplet diffusion in Alq<sub>3</sub> and also show minimal change when reverse bias is applied to the empty traps. However, in Fig. 4(b) we observe that a similar structure using a 8% PtOEP:CBP emission layer fails to show delayed phosphorescence when reverse bias is applied. When reverse bias is absent, the decay lifetime is increased due to the transport of electrons across the 400-Å-thick CBP spacer layer, indicating that in this case hole trapping on PtOEP is significant. Similarly, in Fig. 4(c) the transient response of 6% Ir(ppy)<sub>3</sub>:CBP with a 500-Å-thick diffusion layer also exhibits hole trapping on Ir(ppy)<sub>3</sub>. In contrast, exciton transfer to Ir(ppy)<sub>3</sub> is observed in 6% Ir(ppy)<sub>3</sub>:TPD with a 200-Å-thick diffusion layer; see Fig. 4(d). Here, the observed lifetime of Ir(ppy)<sub>3</sub> is  $\sim 15$   $\mu$ s, significantly longer than its natural radiative decay of  $\sim 1$   $\mu$ s. Taken together with the apparent absence of charge trapping on Ir(ppy)<sub>3</sub> in TPD, this long lifetime indicates that energy transfer from TPD to Ir(ppy)<sub>3</sub> is the rate-limiting step in Ir(ppy)<sub>3</sub> phosphorescence.

All systems exhibit delayed phosphorescence in the absence of reverse bias; however, only (a) PtOEP:Alq<sub>3</sub> and (d) Ir(ppy)<sub>3</sub>:TPD retain delayed phosphorescence in the presence of a strong negative bias. Thus, we conclude that triplet energy transfer is present in these systems but that the other systems, (b) PtOEP:CBP and (c) Ir(ppy)<sub>3</sub>:CBP, are dominated by charge trapping and exciton formation directly upon

the phosphorescent molecule; indeed, the deep HOMO level of CBP makes hole trapping on the guest likely when it is used as a host. In Sec. VII, we discuss the relative merits of trapping and energy transfer as mechanisms for generating very-high-efficiency phosphorescent emission in OLED's. But in the remainder of this and the following section we concentrate on those systems exhibiting energy transfer: notably, PtOEP:Alq<sub>3</sub> and Ir(ppy)<sub>3</sub>:TPD.

In Fig. 4(d), the peak in the delayed phosphorescence of Ir(ppy)<sub>3</sub>:TPD occurs over 100  $\mu$ s after excitation. If we examine the transient of an Ir(ppy)<sub>3</sub>:TPD device where there is no layer separating the exciton-formation interface from the luminescent zones, we find that delayed phosphorescence is absent and that the observed lifetime after electrical excitation is  $15 \pm 2$   $\mu$ s [see Fig. 5(a)]. Except for an initial peak containing some TPD fluorescence, the decay is monoexponential and completely comprised of Ir(ppy)<sub>3</sub> emission. The PL decay of 10% Ir(ppy)<sub>3</sub>:TPD also exhibits long-lived Ir(ppy)<sub>3</sub> emission [see Fig. 5(b)]; however, the PL transient differs in that the initial peak is larger than that found in the EL decay, and no emission is observed from TPD.

The data of Figs. 4(d), 5(a), and 5(b) are to be compared with the natural phosphorescent lifetime of Ir(ppy)<sub>3</sub>, which is only  $\sim 1$   $\mu$ s. As expected from the relative phosphorescent spectra and lifetimes of TPD and Ir(ppy)<sub>3</sub>, these data can be explained by triplets residing for extended periods on TPD

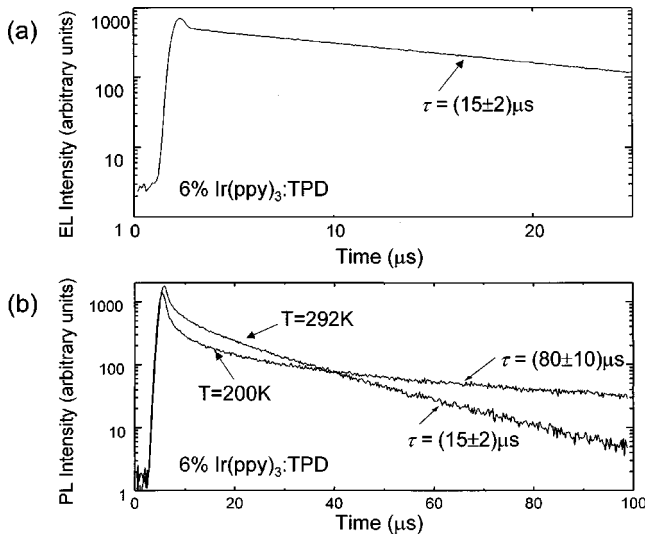


FIG. 5. (a) The electroluminescent response of 8% Ir(ppy)<sub>3</sub> in TPD. The device contains no diffusion layer yet the lifetime of Ir(ppy)<sub>3</sub> in TPD is significantly longer (15  $\mu$ s) than the natural radiative lifetime of Ir(ppy)<sub>3</sub> ( $\sim$ 1  $\mu$ s). The initial peaks in the response is principally due to fluorescence from TPD. (b) The photoluminescent response of 8% Ir(ppy)<sub>3</sub> in TPD at  $T=292$  K and  $T=200$  K. The lifetime increases at low temperatures, consistent with a thermally activated process. However, unlike the EL response, the initial transient in the photoluminescent response is comprised entirely of emission from photoexcited Ir(ppy)<sub>3</sub>.

molecules. The rate of forward transfer ( $k_F$ ) is slow ( $\sim$ 15  $\mu$ s) and dominates the phosphorescent lifetime of Ir(ppy)<sub>3</sub> in TPD. We note that because the observed 15- $\mu$ s Ir(ppy)<sub>3</sub> EL decay is also observed in the PL response, there must be significant populations of triplets in TPD after photoexcitation, i.e.,  $k_R \gg k_F$ . The EL quantum efficiency of Ir(ppy)<sub>3</sub> in

TPD is  $\eta \sim 3\%$ , providing evidence that efficient electrophosphorescence is possible even if it is energetically unfavorable for triplets to reside for an extended duration on the phosphor.

## VI. TRIPLET DIFFUSION IN Alq<sub>3</sub>

Previous work<sup>2,3</sup> has demonstrated the existence of triplet diffusion in Alq<sub>3</sub> and in Figs. 6 and 7 we study the behavior of diffusing triplets as a function of time and distance. Layers consisting of 8% PtOEP:Alq<sub>3</sub> are used to detect the triplets via electrophosphorescence; but in contrast to the other devices grown in this work, here we vary the thickness of the Alq<sub>3</sub> spacer layer and observe the changes in the phosphorescent decay transient. Figure 6 shows the normalized transient responses of PtOEP phosphorescence at  $\lambda = 650$  nm for OLED's with spacer layers of thickness (a) 200  $\text{\AA}$ , (b) 400  $\text{\AA}$ , (c) 600  $\text{\AA}$ , and (d) 800  $\text{\AA}$ . All traces exhibit delayed phosphorescence under reverse bias, demonstrating the presence of triplet diffusion.

These delayed responses are understood as convolutions of the rate of triplet arrival at the phosphorescent sensing layer with the phosphorescent decay of PtOEP. By deconvolving the phosphorescent lifetime of PtOEP from the observed decay, we can therefore extract the triplet-exciton current entering the phosphorescent sensing layer of each device (see Fig. 7). That is, the exciton current is calculated from the data of Fig. 6 by subtracting the initial fluorescent spikes, smoothing, and then deconvolving the phosphorescent decay of PtOEP.

The triplet-exciton current, shown by the data points in Fig. 7, can be fitted to the diffusion equation

$$\frac{d\phi}{dt} = -\frac{\phi}{\tau} + D_T \frac{d^2\phi}{dx^2}. \quad (8)$$

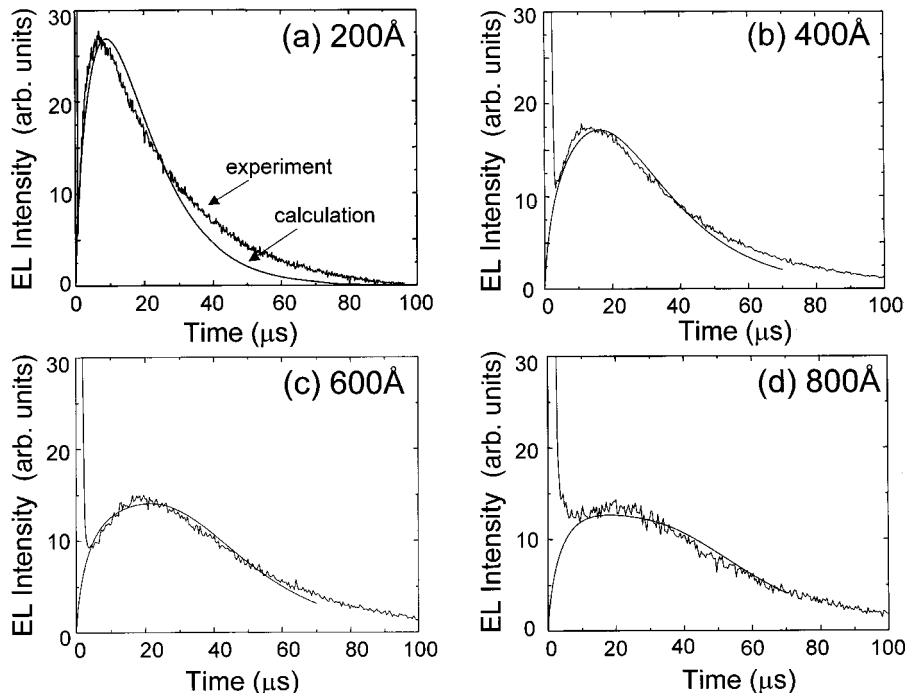


FIG. 6. The normalized, phosphorescent transients for PtOEP in Alq<sub>3</sub> recorded at 650 nm for diffusion distances of (a) 200  $\text{\AA}$ , (b) 400  $\text{\AA}$ , (c) 600  $\text{\AA}$ , and (d) 800  $\text{\AA}$ . Also shown are the calculated transients (smooth curves) based on nondispersive diffusion of triplets given a diffusion coefficient of  $D = (8 \pm 5) \times 10^{-8}$  cm<sup>2</sup>/s, and a triplet exciton lifetime in Alq<sub>3</sub> of  $\tau = 25 \pm 15$   $\mu$ s.

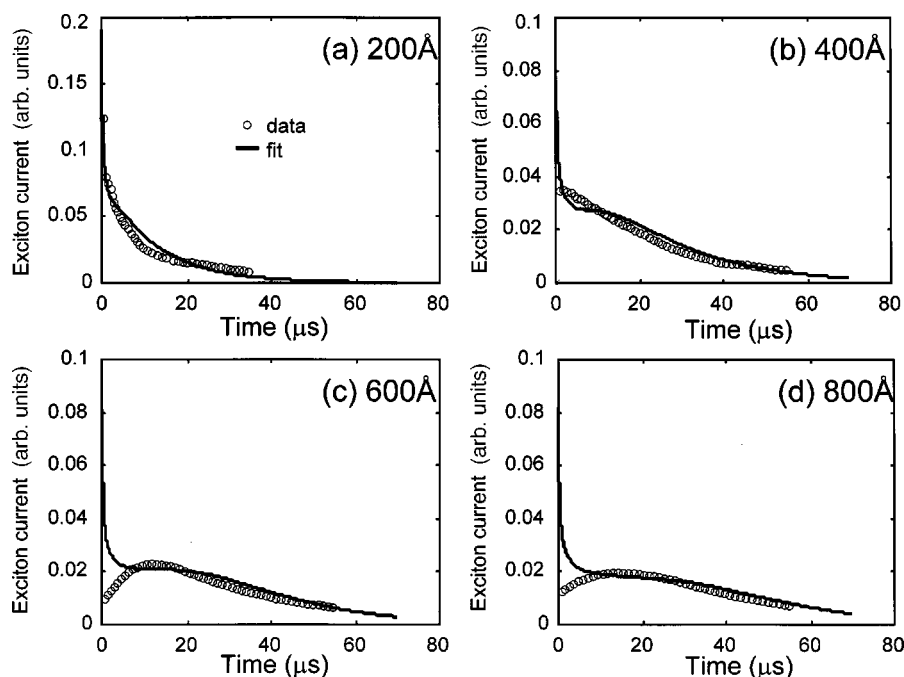


FIG. 7. The exciton current incident in the phosphorescent zone for diffusion distances of (a) 200 Å, (b) 400 Å, (c) 600 Å, and (d) 800 Å (points). The current is calculated (points) by deconvolving the phosphorescent decay of PtOEP from the traces in Fig. 6. Also shown are the best fits assuming nondispersive behavior, assuming that the concentration of exciton formation decreases exponentially with distance from the HTL/ETL interface with a characteristic length of  $L \sim 120$  Å (Ref. 21). The smooth curves in Fig. 6 are calculated from these fits by convolving them with the PtOEP phosphorescent decay.

As shown by the solid lines in Fig. 7, this fit is used to obtain values for the lifetime ( $\tau$ ) of Alq<sub>3</sub> triplets and also their diffusion constant ( $D_T$ ). Finally, as a check, the predicted exciton currents are reconvolved with the PtOEP phosphorescent decay and compared to the measured transients of Fig. 6 (solid lines). For these fits, we assume that the exciton-formation zone is the same in each device and that the exciton concentration decreases exponentially with distance from the HTL interface, with a characteristic length of  $L \sim 120$  Å.<sup>21</sup> The spikes at  $t \rightarrow 0$  observed in the deconvolved exciton currents are due to excess triplets formed within the phosphorescent zone and may indicate the presence of residual charge trapping.

From both Figs. 6 and 7, we find that the simple theory provides a reasonable approximation to the observed transient decays of the PtOEP:Alq<sub>3</sub> system. Nevertheless, given a single value of  $D_T$ , it is impossible to reproduce both the sharp initial increases in the phosphorescent transients and also their long tails. Thus, similar to charge transport, the data provide evidence for dispersive exciton transport, either due to the presence of exciton traps or a distribution in the diffusion coefficient arising from variation in molecular conformations within the amorphous Alq<sub>3</sub> film.

The data fall into two regimes: for short diffusion distances,  $D_T$  determines the observed exciton currents, and at longer distances the currents are limited by the exciton lifetime  $\tau$ . From fits to devices with a spacer layer thickness of 200 or 400 Å, we obtain a diffusion coefficient of  $D_T = (8 \pm 5) \times 10^{-8}$  cm<sup>2</sup>/s, and from fits to the 600- and 800-Å devices, we obtain an exciton lifetime of  $\tau = 25 \pm 15$  μs, taken together to yield a diffusion length of  $L_d = 140 \pm 90$  Å. This is less than the length calculated previously<sup>2</sup> at  $J = 6.5$  mA/cm<sup>2</sup>, however, the current densities applied during

the 200-ns excitation pulses are significantly higher ( $J \sim 2500$  mA/cm<sup>2</sup>). As discussed in Paper II, we expect that increased triplet-triplet annihilation and triplet-charge-carrier quenching at high injection levels causes the observed reduction in diffusion length.

Previously, the single-exciton diffusion coefficient in Alq<sub>3</sub> was measured to be  $D_S = (1.2 \pm 0.8) \times 10^{-5}$  cm<sup>2</sup>/s (Ref. 22) and  $D_S = 2.6 \times 10^{-4}$  cm<sup>2</sup>/s (Ref. 23). The diffusion coefficient of triplets is typically lower than that of singlets since both the donor and acceptor transitions are disallowed.<sup>6</sup>

## VII. CONCLUSIONS

Unlike fluorescent guest-host systems, the phosphorescent systems summarized in Table II do not require energy transfer from guest to host (i.e.,  $\Delta G < 0$ ). Given minimal triplet losses in the host, the only relaxation pathway may be phosphorescence from the guest, and, as is observed in Ir(ppy)<sub>3</sub> in TPD, the overall electroluminescent quantum efficiency of phosphorescent OLED's with  $\Delta G > 0$  can be as high as 3%. In such a system, the excitations reside primarily on the host and are eventually transferred to phosphorescent guest sites prior to emission. Although guest-host combinations with  $\Delta G < 0$  generally exhibit superior performance by minimizing losses at the host, systems with  $\Delta G > 0$  may be useful for high energy triplet emitters such as blue phosphors.

Similar to Ir(ppy)<sub>3</sub> in TPD, triplet diffusion from host to guest is observed for PtOEP in Alq<sub>3</sub>. From transient analyses of exciton transport in Alq<sub>3</sub>, it is likely that the transport is dispersive with behavior similar to charge transport. Nevertheless, in approximating it as a nondispersive system, we obtain a diffusion coefficient of  $D_T = (8 \pm 5) \times 10^{-8}$  cm<sup>2</sup>/s and triplet lifetime of  $\tau = (25 \pm 15)$  μs.

TABLE II. The electrophosphorescent quantum efficiencies and several properties of a range of material combinations.

Guest (lifetime)	Host	$\Delta G$ ( $\pm 0.1$ eV)	Host lifetime	Emission lifetime ( $\mu s$ )	Trapping on guest	EL quantum efficiency
PtOEP ( $110 \pm 10 \mu s$ )	CBP	-0.7	>1 s	$80 \pm 5$	Yes	6%
	Ir(ppy) <sub>3</sub>	-0.5	<0.1 $\mu s$	$80 \pm 5$	?	3%
	TPD	-0.4	$200 \pm 50 \mu s$	$80 \pm 5$	Yes	3%
Ir(ppy) <sub>3</sub> ( $0.8 \pm 0.1 \mu s$ )	Alq <sub>3</sub>	-0.1	$25 \pm 15 \mu s$	$40 \pm 5$	No	3%
	CBP	-0.2	>1 s	$0.4 \pm 0.05$	Yes	8%
	TPD	+0.1	$200 \pm 50 \mu s$	$15 \pm 2$	No	3%
	Alq <sub>3</sub>	+0.4	$25 \pm 15 \mu s$	<0.1	?	<0.1%

All the guest-host systems employing the green phosphor Ir(ppy)<sub>3</sub> exhibit weak triplet confinement on the phosphorescent guest, i.e.,  $\Delta G \sim 0$ . Indeed, reverse transfer from Ir(ppy)<sub>3</sub> to CBP is undoubtedly responsible for some losses in luminescence efficiency and the decrease in phosphorescent lifetime from  $\sim 0.8$  to  $\sim 0.4 \mu s$ . In spite of this, external quantum efficiencies as high as 8% have been obtained from Ir(ppy)<sub>3</sub> doped in CBP.<sup>4</sup> As confirmed by the transient studies here, these efficiencies are possible because a majority of excitons are formed directly on Ir(ppy)<sub>3</sub> following charge trapping. The deep HOMO level of CBP, in particular, appears to encourage hole trapping on phosphorescent guests. But there remains significant room for improvement, and at least a further doubling of phosphorescent efficiency should be possible given the right host material.

In the following paper we address one of the paradoxes of phosphorescent OLED's: the need for high concentrations of phosphorescent guests despite the apparently long diffusion

lengths of triplets. It is determined that mobile triplets tend to annihilate, and therefore it is preferable to transfer them rapidly to phosphorescent guests where they are trapped. Since triplet transport is a short-range interaction, transfer rates are increased at high guest molecule concentrations when almost every host molecule has at least one neighboring guest. In this way, high concentrations of phosphorescent guest molecules may minimize triplet-triplet annihilation. Thus, the ideal guest-host combination should exhibit both triplet confinement and encourage the formation of triplets directly on the guest.

#### ACKNOWLEDGMENTS

This work was supported by Universal Display Corporation, the Defense Advanced Research Projects Agency, the Air Force Office of Scientific Research, and the National Science Foundation MRSEC program.

<sup>1</sup>M. Klessinger and J. Michl, *Excited States and Photochemistry of Organic Molecules* (VCH, New York, 1995).

<sup>2</sup>M. A. Baldo, D. F. O'Brien, M. E. Thompson, and S. R. Forrest, *Phys. Rev. B* **60**, 14 422 (1999).

<sup>3</sup>M. A. Baldo, D. F. O'Brien, Y. You, A. Shoustikov, S. Sibley, M. E. Thompson, and S. R. Forrest, *Nature (London)* **395**, 151 (1998).

<sup>4</sup>V. Cleave, G. Yahiolglu, P. Le Barny, R. Friend, and N. Tessler, *Adv. Mater.* **11**, 285 (1999).

<sup>5</sup>M. A. Baldo, C. Adachi, and S. R. Forrest, *Phys. Rev. B* **62**, 10 967 (2000).

<sup>6</sup>M. Pope and C. Swenberg, *Electronic Processes in Organic Crystals* (Oxford University Press, Oxford, 1982).

<sup>7</sup>D. L. Dexter, *J. Chem. Phys.* **21**, 836 (1953).

<sup>8</sup>G. L. Closs, M. D. Johnson, J. R. Miller, and P. Piotrowiak, *J. Am. Chem. Soc.* **111**, 3751 (1989).

<sup>9</sup>G. L. Closs and J. R. Miller, *Science* **240**, 440 (1988).

<sup>10</sup>R. A. Marcus, *J. Chem. Phys.* **24**, 966 (1955).

<sup>11</sup>T. Forster, *Discuss. Faraday Soc.* **27**, 7 (1959).

<sup>12</sup>M. A. Baldo, M. E. Thompson, and S. R. Forrest, *Nature (London)* **403**, 750 (2000).

<sup>13</sup>S. R. Forrest, *Chem. Rev.* **97**, 1793 (1997).

<sup>14</sup>M. A. Baldo, S. Lamansky, P. E. Burrows, M. E. Thompson, and S. R. Forrest, *Appl. Phys. Lett.* **75**, 4 (1999).

<sup>15</sup>D. F. O'Brien, M. A. Baldo, M. E. Thompson, and S. R. Forrest, *Appl. Phys. Lett.* **74**, 442 (1999).

<sup>16</sup>I. G. Hill and A. Kahn, *J. Appl. Phys.* **86**, 4515 (1999).

<sup>17</sup>H. Ishii, K. Sugiyama, E. Ito, and K. Seki, *Adv. Mater.* **11**, 605 (1999).

<sup>18</sup>V. Bulovic, V. B. Khalfin, G. Gu, P. E. Burrows, D. Z. Garbuzov, and S. R. Forrest, *Phys. Rev. B* **58**, 3730 (1998).

<sup>19</sup>D. Z. Garbuzov, V. Bulovic, P. E. Burrows, and S. R. Forrest, *Chem. Phys. Lett.* **249**, 433 (1996).

<sup>20</sup>R. Ballardini, G. Varani, M. T. Indelli, and F. Scandola, *Inorg. Chem.* **25**, 3858 (1986).

<sup>21</sup>J. Kalinowski, N. Camaioni, P. Di Marco, V. Fattori, and A. Martelli, *Appl. Phys. Lett.* **72**, 513 (1998).

<sup>22</sup>I. Sokolik, R. Priestley, A. D. Walser, R. Dorsinville, and C. W. Tang, *Appl. Phys. Lett.* **69**, 4168 (1996).

<sup>23</sup>C. W. Tang, S. A. VanSlyke, and C. H. Chen, *J. Appl. Phys.* **65**, 3610 (1989).